T. Yilmaz, R. Foster and Y. Hao, “Broadband Tissue Mimicking Phantoms and a Patch Resonator for Evaluating Non-invasive Monitoring of Blood Glucose Levels”, *IEEE Trans. Ant. Prop.*, vol. 62, no. 6, pp. 3064-3075, June 2014.

This post-acceptance version of the paper is essentially complete, but may differ from the official copy of record, which can be found at the following web location (subscription required to access full paper): http://dx.doi.org/10/1109/TAP.2014.2313139.

Broad-Band Tissue Mimicking Phantoms and a Patch Resonator for Evaluating Non-Invasive Monitoring of Blood Glucose Levels

Tuba Yilmaz, *Student Member, IEEE,* Robert Foster, *Member, IEEE,* and Yang Hao, *Fellow, IEEE*

***Abstract*—Wide-band tissue mimicking phantoms (TMPs) are presented that replicate the dielectric properties of wet skin, fat, blood, and muscle tissues for the 0.3 GHz to 20 GHz frequency range. The TMPs reflect the dielectric properties with maximum deviations of 7.7 units and 3.9 S/m for relative dielectric constant and conductivity, respectively, for the whole band. The dielectric properties of the blood mimicking material are further investigated by adding realistic glucose amounts and a Cole-Cole model used to compare the behavior with respect to changing glucose levels.**

In addition, a patch resonator was fabricated and tested with the four-layered physical phantom developed in house. It was observed that the input impedance of the resonator is sensitive to the changes in the dielectric properties and, hence, to the realistic glucose level changes in the blood layer.

***Index Terms*—on-body RF Devices, Cole-Cole Fitting, Tissue Mimicking Phantoms, Patch Resonator, Blood Glucose Levels**

I. Introduction

Within the last few decades, changes in lifestyle and nutrition made diabetes mellitus one of the most commonly seen diseases among chronic conditions. Complications of diabetes can only be managed with frequent monitoring of blood glucose levels (BGL); thus, there is a need to monitor BGL non-invasively and continuously. There are 1.3 million people with diabetes in England and further complications of diabetes include kidney failure, blindness in adults, and limb amputation. Also, diabetes significantly increases the risk of stroke and coronary heart disease [1]. Currently, diabetes is managed by ambulatory monitoring of BGL. The patient withdraws blood with a lancet and places a drop of blood on a pre-treated strip, which then inserted into a digital monitor. However, such kits are invasive and do not provide continuous monitoring.

Radio frequency (RF) techniques in the literature are mostly focused on telemetry and BGL sensing is usually performed with a chemical sensor [2]–[4]. A limited number of studies have been published employing RF techniques for sensing changes in BGL. One of the studies published in this area is given in [5] and [6]; in this work, a two-port spiral resonator is presented. The S_{21} response of the resonator is tracked by placing the resonator radiating towards the tissue while the BGL is fluctuated with a procedure named the *Soda Test*. The experiments are performed with humans without *a priori* knowledge of the dielectric properties of the blood. The study is aimed to relate the glucose levels with the output of the spiral resonator. It is noted, however, that the experience of the authors has found that the pressure between phantom and resonator can have an effect on the performance of the spiral resonator. Investigation of this phenomenon by the authors is on-going.

An ultra-wide band (UWB) antenna was presented in [7] and the return loss response of the antenna was tracked. The study reported significant changes in the simulated return loss response of the UWB antenna. However, the dielectric property data given to the simulation software was derived from [8]. [8] reports the dielectric property change in erythrocyte membranes. However, the International Federation of Clinical Chemistry and Laboratory Medicine recommends the use of plasma glucose levels during blood glucose tests, which is 11% lower than the whole blood glucose levels [9]. The erythrocyte membranes are not representative of either whole blood or plasma glucose levels. Hence, there is some uncertainty regarding the interpretation of these results.

In order to fully understand the potential of an RF application, the relationship between the dielectric property change and glucose level change of blood should be established. Previously reported studies suggest that the dielectric properties of blood depend on the changes in the components of blood; thus, the dielectric properties of the blood can be changed with the alterations in blood glucose levels [8]. These findings imply that an RF application can be used to detect such changes and blood glucose level assessment can be accomplished by means of RF applications. A recently reported study suggests that the dielectric properties of blood decrease as the blood glucose levels are increased [10]. The normal range for BGL is 72 mg/dl to 216 mg/dl; however, previously reported studies carried out measurements with very large amounts of glucose. In [10], the dielectric properties of blood plasma are measured with varying glucose levels from 0 mg/dl to 16000 mg/dl, with an increment of 250 mg/dl, which is much higher than the normal blood glucose range.

In [11], a study was performed with real blood samples collected from 10 patients, with BGL ranging from 87 mg/dl to 330 mg/dl in the 1 GHz to 10 GHz frequency band. In [12], dielectric properties of the blood mimicking phantom materials were reported between 0.5 GHz to 3 GHz. However, these studies do not provide detailed information and conclusions regarding the change of permittivity within the range of realistic BGL change.

The authors are with the School of Electronic Engineering and Computer Science, Queen Mary, University of London, London, E1 4NS. Email yang.hao@eecs.qmul.ac.uk

Manuscript received October ??, 2012.

This interest in using RF techniques for blood sugar level monitoring has, to the authors' knowledge, not yet examined the sensitivity issues related to normal BGL values and the associated dielectric properties. In addition, there are trade-offs regarding the RF resonator (e.g., size, sensitivity, operating frequency) that remain poorly understood. This study seeks to gain insight into these issues. The approach taken was to develop wide-band tissue mimicking phantoms that would be suitable for this and future investigations into resonators, where the same phantoms could be used with resonators in different frequency bands. Furthermore, these wide-band TMPs were used in this work to investigate the likely sensitivity requirements of the resonators, due to the limited changes in resonator behavior expected from small, realistic changes in glucose level (i.e., changes within the normal range for humans). Hence, the contributions reported in this paper concern two vital issues that have not been reported in detail in previous studies, that are necessary to understand the viability of RF methods for BGL monitoring:

1) establishing a clear relation between the dielectric properties and the realistic glucose levels of the blood mimicking phantom materials, in an extremely wide frequency range; and
2) performing controlled patch resonator experiments with a minimum effect from the measurement conditions, to allow some assessment of the sensitivity requirements under realistic conditions.

A patch resonator was designed for the investigation into sensitivity requirements. It was optimised through simulation to operate in the 2.4-2.48 GHz ISM band when placed with the radiating element against the four-layered tissue phantom; then, by decreasing the relative dielectric constant of the blood layer, the simulated response of the resonator was analyzed. Experiments were performed with physical phantoms for cross-validation, and in order to study the effect of blood glucose on the dielectric properties of the blood: for these, tissue mimicking materials were fabricated and characterized. Powdered dextrose (glucose) was added to the blood mimicking material and dielectric property measurements were performed. A Cole-Cole analysis was performed to quantify the dielectric property change in the blood mimicking material. The resonator was tested with the four-layered tissue mimicking material and the simulations were validated by repeating the measurements using blood mimicking materials with differing amounts of glucose content.

Section II provides the recipes and characterization of the tissue mimicking materials over the frequency range 0.3-20 GHz. The design of the patch resonator and the experimental methodology for testing of the resonator are also explained in Section II. Analysis methods are presented in Section III; the results are presented in Section IV. Finally, conclusions are drawn in Section V.

II. Design and Experimental Methodology

A. Tissue Mimicking Materials

1) Characterization of Tissue Mimicking Materials: Different types of tissue mimicking materials have been proposed in the literature to test the performance of implantable telemetry devices, breast cancer imaging techniques, and to evaluate specific absorption rates (SAR) [13]–[15]. Tissue mimicking materials, depending on the application, can be characterized in solid, liquid, or semi-solid forms. The liquid forms are the simplest TMP material type and have been used in the literature to test antennas and resonators for proper functioning (e.g., [16], [17]). The semi-solid tissue phantoms are widely used for testing of bio-telemetry and imaging tools. In this paper, semi-solid oil-in-gelatine dispersion phantoms using off-the-shelf ingredients have been proposed to test the patch resonator. The following describes the approach taken to make the TMPs, with the effects of each ingredient described and potential problems to watch for, for those unfamiliar with physical phantoms.

TABLE I
Ingredients of Broad-Band (0.2 - 20 GHz) Tissue-Mimicking Phantoms

Ingredient (g)	Wet Skin	Fat	Blood	Muscle
Water	230.0	57.4	230.0	230.0
Gelatine	34.1	15.0	34.1	34.1
NaCl	1.4	0.0	1.2	1.2
Oil	75.0	329.6	15.0	35.0
detergent_1	40.0	0.0	40.0	40.0
detergent_2	0.0	10.0	0.0	0.0
food coloring	1.3	0.0	0.0	1.3

Using results from the literature and the guided trial-and-error approach, wet-skin, fat, blood, and muscle mimicking phantoms were developed [15]–[18]. The existing results in the literature may be summarized as: among all ingredients, water has the highest relative dielectric constant values; adding sodium chloride (NaCl) to a mixture increases the conductivity; adding oil to the mixture decreases both the relative dielectric constant and the conductivity; and gelatine can be used as a solidifying agent.

Considering the existing knowledge for high relative dielectric constant materials, such as so-called high water content tissues like blood, the de-ionized water percentage should be higher compared to the fat tissue. Similarly, for low water content tissues, the oil percentage in the mixture should be higher. Such materials can be mimicked by using other ingredients, such as triton TX-100 instead of oil [13], [16]; however, including oil in the mixture allows the dielectric properties of the biological tissues to be mimicked over an extremely wide frequency range. Note that, in this work, oil refers to pure vegetable oil.

Previously, similar recipes of oil-in-gelatine TMPs have been proposed in the literature [14], [18]. However, these recipes include chemicals to lengthen the shelf-life of the TMP. Adding chemicals to the recipe complicates the fabrication procedure and increases the cost. In addition, such chemicals are only available from specific providers. Therefore, we used a small number of key ingredients, given in Table I, that can be obtained from grocery stores. Note that the food coloring is optional, since it has been included to identify the different tissues when stacked on top of one another. The

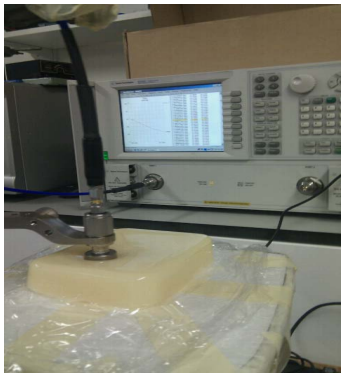

Fig. 1. Dielectric property measurement set-up with Agilent's high temperature dielectric probe.

difference between detergentt_1 and detergent$_2$ is explained in the appendix.

The fabrication of the physical phantoms requires the following steps:

1) mix the gelatine and 100 g de-ionized water in a beaker;
2) cover the beaker with cling film and heat the mixture up to 80 °C in a hot water jacket or in a double boiler;
3) leave the mixture to cool until 35 °C;
4) add the remaining room temperature deionized water and NaCl whilst stirring the mixture slowly;
5) add the room temperature dish-washing detergent to the mixture and keep stirring slowly;
6) when the mixture reaches 28 °C, add room temperature oil and keep stirring slowly until the mixture become homogeneous. At this point the color of the mixture changes to white. Adding food coloring at this point allows the phantoms to be distinguished;
7) pour the homogeneous mixture into containers and leave it to solidify over night.

Avoiding air bubbles while making the tissue mimicking phantoms is very important. Thus, the mixture should be handled with care; to avoid micro bubbles, the mixture can be filtered at the last step. If air bubbles form in the mixture, they will fly to the top of the phantom and form a non-smooth surface. Although it is impossible to avoid air bubbles completely, they can be minimized by stirring the mixture slowly.

After the phantom mixtures had solidified, dielectric property measurements were carried out with Agilent's open ended high temperature dielectric probe. The dielectric probe has a flange with a diameter of 19.0 mm and the aperture size is 3.5 mm in diameter. To ensure a good contact between probe and the sample, the probe was immersed into the sample. The gel-like nature of the sample allowed the immersion. Measurements were taken at room temperature (23 °C). All dielectric property measurements were carried out with samples having a minimum thickness of 20 mm.

Dielectric property measurements were taken from different points on the top and bottom surfaces of the phantoms. First, the measurements from the top were collected from at least five different points. Two measurements were taken at each point: after collecting the first measurement at a given point, the probe was left in contact with the phantom for three to five minutes and another measurement taken from the same point. The same measurement routine was repeated for the bottom surface of the phantom. The measurement set-up is shown in Fig. 1. Dielectric property measurement results are given in Section IV.

TABLE II
BLOOD MIMICKING MATERIAL WITH CORRESPONDING GLUCOSE INDEX

Dextrose (g)	Glucose (mmol/l)	Glucose (mg/dl)
0.14	4	72
0.24	7	126
0.34	9	162
0.44	12	216

2) Dielectric Property Measurements of Blood Mimicking Material with Varying Realistic Blood Glucose Levels: This section describes the experimental method used to quantify the dependence of the dielectric properties of the blood mimicking materials to the blood glucose levels. To this end, an oil-in-gelatin dispersion blood mimicking material was made, using the recipe given in Table I. The blood mimicking material was divided into five 200 ml beakers, each beaker containing around 200 grams of blood mimicking phantom. Next, 0 g, 0.14 g, 0.24 g, 0.34 g, and 0.44 g of powdered dextrose (glucose) was added to the beakers, respectively, at 28 °C. Corresponding mmol/l and mg/dl values for glucose are given in Table II. The phantoms were poured into 78 mm by 111 mm containers to a thickness of 24 mm. The samples were left overnight to solidify. Five samples in total were prepared. Dielectric property measurements were taken within 18 to 30 hours of phantom characterization with Agilent's open ended high temperature dielectric probe, following the dielectric property measurement routine described in Section II-A1.

Dielectric property measurements were collected from the top and bottom sides of the phantoms from at least five points on each side and two measurements collected from each point. The total number of measurements collected from all the phantom samples was 107, with 2500 data points across the frequency range for each measurement.

B. Design of Patch Resonator

In order to obtain some initial insights into the use of resonators for BGL monitoring, an on-body patch resonator was designed to operate in the 2.40-2.48 GHz ISM band when radiating towards the tissue. The resonator was designed using CST Microwave Studio software, with a four-layered (skin, fat, blood, and muscle) digital phantom placed above the resonator as a superstrate to represent the lossy biological tissue. All tissues have planar dimensions of 127 mm by 127 mm, and the thicknesses of the phantoms are given in Table III. The phantoms are given non-dispersive dielectric properties of the biological tissues at the designed operation frequency (2.45 GHz), also given in Table III [19], [20].

The configuration of the resonator is given in Fig. 2 and the dimensions are given in Table IV. The resonator is printed on Rogers 3210 substrate with ε_r =10.2 and a dissipation

TABLE III
DIELECTRIC PROPERTIES AND THICKNESSES OF THE DIGITAL PHANTOMS AT 2.45 GHZ

Tissue Type	Permittivity	Conductivity (S/m)	Thickness (mm)
Wet Skin	42.923	1.562	1.0
Fat	5.283	0.103	1.0
Blood	58.347	2.502	2.5
Muscle	52.791	1.705	15.1

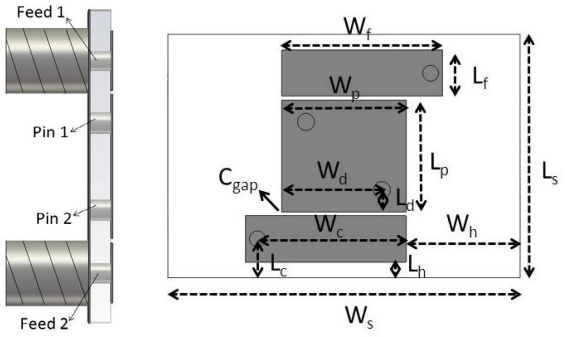

(a) (b)

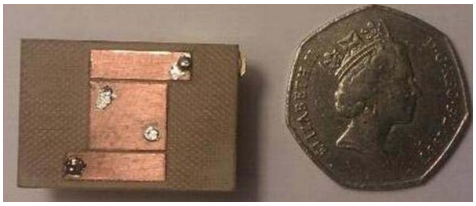

(c)

Fig. 2. Patch Resonator: (a) side view; (b) top view; (c) printed resonantor.

factor of 0.0027 at 10 GHz. The high dielectric constant of the substrate enables the miniaturization of the resonator. The size of the substrate is 29 mm by 20 mm, which is comparable to a conventional implantable antenna. Two shorting via pins are used to connect the patch to the ground plane symmetrically. The shorting vias enabled further miniaturization of the resonator. The patch resonator is a two-port structure and the energy is capacitively coupled to the patch with two feeding lines. The feeding lines are fed with SMA connectors. The return loss measurement and simulation results for both air and tissue medium are given in Section IV.

C. Testing of the Resonator with Tissue Mimicking Materials

In this section, the resonator is tested with tissue mimicking materials. Dextrose was added to the blood mimicking material

TABLE IV
DIMENSIONS OF THE PATCH RESONATOR

Parameter	Value (mm)	Parameter	Value (mm)	Parameter	Value (mm)
W_s	29.00	W_h	9.365	L_d	1.8
W_f	13.27	L_p	9.2	L_f	3.8
W_p	10.27	L_s	20.0	L_h	1.3
W_c	12.27	L_c	3.2	C_{gap}	47.0
W_d	8.27				

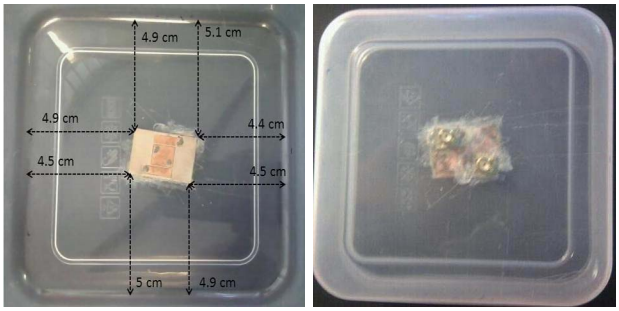

(a) (b)

Fig. 3. Resonator mounted at the bottom of the container: (a) top view; (b) bottom view.

(a) (b)

Fig. 4. Patch resonator: (a) four-layered tissue placed on top of the resonator; (b) measurement set-up.

(BMM) in different indexes, which correspond to real values of glucose in human blood. The response of the resonator was recorded while the BMM layer was replaced with another BMM layer containing a different amount of dextrose. The aim of this experiment was to examine the effect of dextrose change on the response of the resonator.

The fabricated patch resonator was mounted at the bottom of a container. The container had dimensions of 127 mm by 127 mm. During the fabrication of the resonator, SMA coaxial feeds were soldered with a slight angle (i.e., the resonator was tilted 1.98° upwards on the longer side of the substrate); thus, the resonator was tilted up when mounted to the container. The distances from the edges of the container were measured and are given in Fig. 3.

Wet skin, fat, blood, and muscle mimicking materials were made using the recipes and fabrication process given in Section II-A1. Four samples of BMM were fabricated and 0.24 g, 0.34 g, and 0.44 g of dextrose was added to three of the BMM samples, respectively. The wet skin mimicking material was poured in to the container with the resonator mounted at the bottom with 1 mm thickness from the top of the resonator. The other phantoms were poured into identical containers with thicknesses of 1 mm, 2.5 mm, and 15 mm for fat, blood, and muscle mimicking materials, respectively. BMM phantoms with different dextrose index values were also poured in identical containers with a 2.5 mm thickness.

The fat, blood, and muscle layers were placed on top of the wet skin layer and the S-parameter response of the resonator

TABLE V
FEASIBLE SOLUTION SPACE GIVEN TO THE COLE-COLE PARAMETERS IN PSO ALGORITHM

Parameter	ε_∞	$\Delta\varepsilon_n$	τ_n (ps)	α_n	σ_i (S/m)
Minimum	2	2	7	0	0.01
Maximum	6	70	14	1	3

collected, with the blood layer using one from the set of blood mimicking materials. The measurement set-up is shown in Fig. 4.

III. ANALYSIS OF THE COLLECTED DATA

A. Dielectric Property Analysis of Blood Mimicking Phantoms

The collected data from blood mimicking materials with different dextrose index were analyzed in two steps. The first step was the elimination of the poor data. To do this, the measured dielectric properties, for one phantom at a time, were plotted in MATLAB and plots deviating vastly from the majority of measurements were eliminated. This led to 12 out of 107 measurements being eliminated. The discrepancy between the eliminated measurements and the remaining data is attributed to poor physical contact between the semi-solid opaque phantoms. The probe employed for dielectric spectroscopy has a flange which blocks the visual inspection of the contact with the sample, making proper contact difficult to verify.

The second step was to minimize the parameters of the remaining data (95 measurements) for comparison with respect to glucose index, because the collected data contains over a million data points. To this end, a single pole Cole-Cole model was used to express the measured dispersive dielectric properties as a function of frequency. Cole-Cole fitting has been used a number of times in the literature, to compare the dielectric properties of biological tissues, as it expresses the measured data with a compact equation and allows comparisons to be made of the variations of dielectric properties in biological tissue due to the changes in water content, heat, and glucose level [21]–[24]. It has been also shown [23] that the single pole Cole-Cole fitting is more efficient than two pole Cole-Cole fitting, because the number of parameters is smaller and the single pole fitting represents the measured data just as well as two pole fitting. The Cole-Cole equation is given by

$$\varepsilon_\omega = \varepsilon_\infty - \sum_n \frac{\Delta\varepsilon_n}{1+(j\omega\tau_n)^{(1-\alpha_n)}} + \frac{\sigma_i}{j\omega\varepsilon_0} \qquad (1)$$

where ω is the angular frequency and ε_∞, $\Delta\varepsilon_n$, τ_n, α_n, σ_i are the Cole-Cole parameters.

The Cole-Cole parameters were found with particle swarm optimization (PSO) [24], [25]. PSO is a heuristic algorithm that returns all Cole-Cole variables by minimizing the fitness function. The fitness function of the PSO was chosen as the Euclidean distance [26] between the raw data input and the Cole-Cole equation output. The equation for Euclidean distance is given in (2):

$$e = \frac{1}{N}\sum_{i=1}^{N}\left[\left(\frac{\varepsilon'_{\omega_i}-\hat{\varepsilon}'_{\omega_i}}{median\left[\varepsilon'_{\bar{\omega}_i}\right]}\right)^2 + \left(\frac{\varepsilon''_{\omega_i}-\hat{\varepsilon}''_{\omega_i}}{median\left[\varepsilon''_{\bar{\omega}_i}\right]}\right)^2\right] \qquad (2)$$

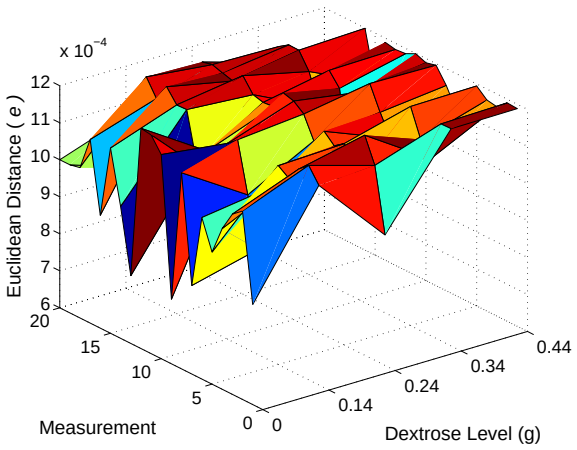

Fig. 5. Euclidean distance from the PSO algorithm's output.

where ε'_{ω_i} and ε''_{ω_i} are the real and imaginary part of measured dielectric properties. $\hat{\varepsilon}'_{\omega_i}$ and $\hat{\varepsilon}''_{\omega_i}$ represent the output of the Cole-Cole equation for the real and imaginary part of the dielectric properties, respectively, and N is the number of points picked across the frequency range of 0.3 GHz to 20 GHz (2500 for this study). The PSO algorithm stops and returns values for the five set of parameters if the Euclidean distance is smaller than the threshold of 0.00012. The pre-determined feasible solution space given to the parameters in the algorithm is shown in Table V.

To verify the validity of Cole-Cole fitting, the Euclidean distance for each fitting was computed, shown in Fig. 5. The number of particles chosen in the PSO algorithm was 30. The algorithm would end after 500 iterations if the threshold were not reached before this point. Note that an additional measurement was excluded, since the Cole-Cole equation could not be fitted to the measurement; thus, 13 measurements in total were excluded. The solutions were reached within 10 to 150 iterations.

B. Input Impedance Analysis of the Resonator

From the literature, it is known that an increase in BGL decreases the relative dielectric constant of blood. To study this effect in terms of the response of the patch resonator, simulations were performed where the relative dielectric constant of the blood layer in a four-layered digital phantom was decreased and the response of the resonator was observed. Firstly, the return loss response was observed, with the resonator was operating at 2.4512 GHz; when the relative dielectric constant was decreased by 2, the operation frequency remained unchanged. From reported studies, we can conclude that the relative dielectric constant alterations at 2.45 GHz is lower than 2 within the range of 4–12 mmol/dl change in blood. Thus, the relative dielectric constant change can not be sensed with the current structure at 2.45 GHz when only tracking the resonance frequency. However, we observed a mismatch at return loss response when the relative dielectric constant of blood layer was changed. To this end, the input impedance of

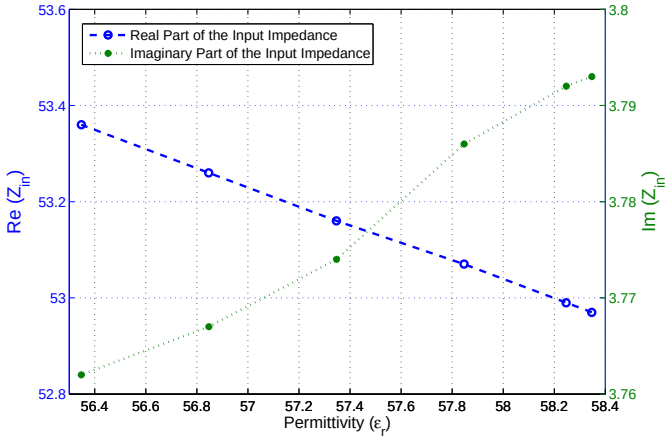

Fig. 6. Simulated change of input impedance with respect to change in blood layer relative dielectric constant.

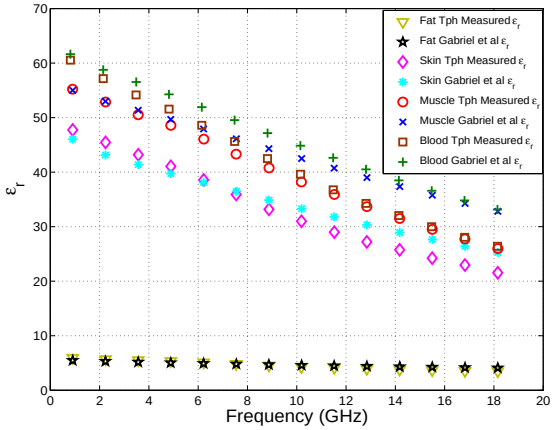

Fig. 7. Relative dielectric constant measurements and literature data [20] comparison for fat, $skin_{wet}$, $muscle$,and $blood$ mimicking materials.

the resonator was calculated from the Z parameter response of the resonator:

$$Z_{in} = Z_{11} - \frac{Z_{12}Z_{21}}{Z_{22} + Z_L} \tag{3}$$

Z-parameters were calculated with CST Microwave Studio, and the load impedance Z_L was considered matched ($50\ \Omega$). The change of input impedance of the resonator with the decrease in relative dielectric constant of the blood layer is given in Fig. 6. The real part of the input impedance is increasing as the relative dielectric constant is decreasing. On the other hand, the imaginary part of the input impedance is decreasing as the relative dielectric constant is decreasing. Note that the input impedance is calculated at 2.4512 GHz.

For the experiment proposed in Section II-A2, the input impedance was calculated from the recorded S-parameter response. First, the S-parameters were converted to Z-parameters; next, the input impedance was calculated using (3). The results are given in Section IV-C.

IV. Results and Discussion

A. Dielectric properties of the Tissue Mimicking Materials

The measured relative dielectric constant and conductivity data for each TMP material sample was averaged and plotted versus frequency, and also compared with the existing literature data [20]; see Fig. 7 and Fig. 8, respectively. Also, the measured dielectric properties of the blood mimicking phantom with varying dextrose levels are given in Fig 9 and Fig 10, for relative dielectric constant and conductivity, respectively.

It is clear that, in general, the agreement between phantoms and the literature is good at low frequencies and that the error increases with frequency. This reflects the difficulty in obtaining wide-band behavior in physical phantoms. The fat phantom shows the best match of the four tissue types.

The measured data is compared by calculating the mean squared error (MSE) with respect to the existing literature data [20] for biological tissues over the extremely wide frequency range 0.3 GHz to 20 GHz. The MSE for relative dielectric

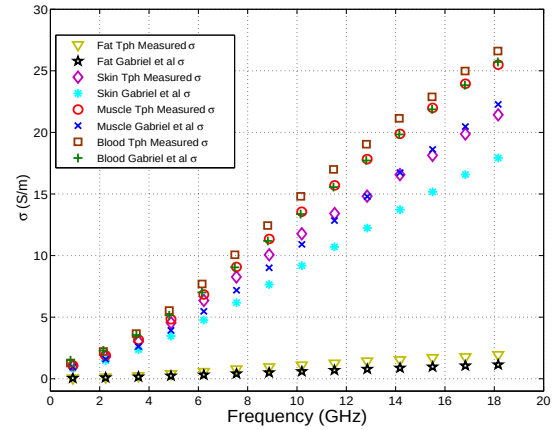

Fig. 8. Conductivity measurements measurements and literature data [20] comparison for fat, $skin_{wet}$, $muscle$,and $blood$ mimicking materials.

constant for $skin_{wet}$, fat, $blood$ (with no dextrose), and $muscle$ are 6.87, 0.21, 25.38, and 21.14, respectively. The MSE for the conductivity measurements are 5.97 S^2/m^2, 0.29 S^2/m^2, 1.12 S^2/m^2, and 6.21 S^2/m^2, for $skin_{wet}$, fat, $blood$, and $muscle$, respectively. From the MSE values, we can conclude that the dielectric properties of the proposed tissue phantoms agree well with the literature data. The MSE values for fat is lower than the rest of the values. This is due to the low water, high oil content of the fat mimicking material. As the oil content increases, the tissue phantoms shows a smooth variation over the frequency range. However, for high water content tissues, as the frequency increases the dielectric property variation tends to change rapidly.

In [18], comparisons are made between their proposed phantoms and tissue properties from [20]. In particular, fat, muscle and wet-skin mimicking materials are compared to their TMP materials with various proportions of oil. They compare fat tissue with 80% oil over the 0.5–20 GHz band. From the reported graphs in [18], the difference with respect to reported literature data [20] for relative dielectric constant

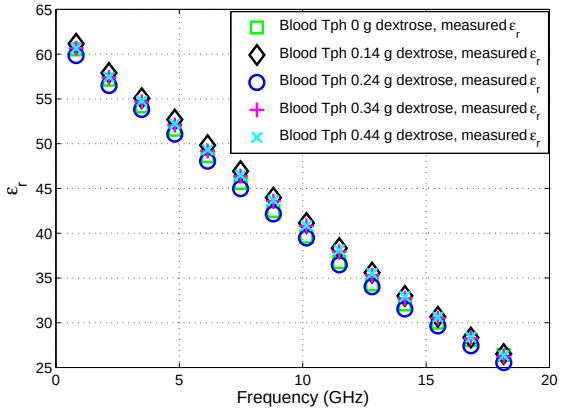

Fig. 9. Relative dielectric constant measurements of blood mimicking material with 0, 0.14, 0.24, 0.34, and 0.44 g dextrose.

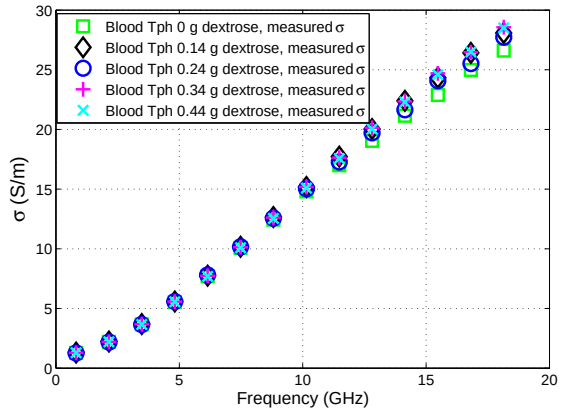

Fig. 10. Conductivity measurements measurements of blood mimicking material with 0, 0.14, 0.24, 0.34, and 0.44 g dextrose.

and conductivity is around 2 units and 1 S/m, respectively. In this study, the difference between our fat mimicking material, which also includes 80% oil, and the reported data on fat tissue is less than 0.9 units and 1 S/m for relative dielectric constant and conductivity, respectively, for the whole 0.3–20 GHz frequency range.

The wet skin mimicking material in this work was composed with 19% oil; the maximum relative dielectric constant and conductivity difference between the literature and measured data is 1.1 units and 3.86 S/m, respectively. In [18], the maximum difference between the 20% oil content TMP material and literature data on wet skin is 4-5 units and 3 S/m, for relative dielectric constant and conductivity, respectively. In [14], a comparison between 30% oil TMP material and $skin_{wet}$ tissue is given up to 6 GHz; the maximum difference is 4 units and 0.7 S/m, for relative dielectric constant and conductivity, respectively.

For the muscle in [18], the maximum difference between the 10% oil TMP material and literature data for relative dielectric constant and conductivity is 8 units and 5 S/m, respectively. For the muscle TMP material in this work the minimum differences are 7.7 units and 3.9 S/m, respectively.

TABLE VI
COLE-COLE PARAMETERS OF MEDIAN CURVES FOR REALISTIC DEXTROSE LEVELS

Parameter	0 g	0.14 g	0.24 g	0.34 g	0.44 g
ε_∞	3.41	2.24	2.67	3.62	3.26
$\Delta\varepsilon_n$	57.13	59.31	56.6	57.56	56.79
τ_n (ps)	11.29	11	11.12	10.85	10.71
α_n	0.09	0.07	0.04	0.05	0.04
σ_i (S/m)	1.05	1.08	1.03	1.05	1.07

From these comparisons with the previously published data on oil-in-gelatine dispersion TMP materials, we can state that phantoms presented in this work mimic the dielectric properties of the $muscle$, $skin_{wet}$, and fat tissues with an acceptable error range, but have an advantage by using fewer ingredients; the trade-off is the probable reduction in the lifetime of the phantoms due to the lack of a preservative in the recipe, though the extent of this has not been investigated at this point.

In addition, this work also presents a comparison between dielectric properties of the blood and blood TMP material; the difference between these is less than 7 units and 1.6 S/m for the whole frequency range. Note that the blood phantom has 4.6% oil content. The validity of the other TMP materials, based on the above comparisons, suggests that the blood TMP material can be used for the whole frequency range. If one desires a better match at higher frequencies for the blood mimicking phantom, the water percentage at the phantom can be increased. It is also worth noting that these recipes can be optimised for high accuracy in narrow frequency bands.

B. Cole-Cole Analysis of the Blood Mimicking Materials with Different Glucose Index

The median values of the measured dielectric properties are calculated at each frequency for the five samples of blood mimicking material, categorized as 0 g, 0.14 g, 0.24 g, 0.34 g, and 0.44 g of dextrose index. Cole-Cole parameters are fitted to the median of the each phantoms; thus, five fittings are performed in total. In order to show the validity of the Cole-Cole fitting, the median of the 0 g dextrose blood mimicking material and fitted Cole-Cole models are shown in Fig. 11 as an example. Calculated Cole-Cole parameters for each phantom sample are shown in Table VI. The method employed to retrieve the Cole-Cole parameters is described in Section III-A. Next, the Cole-Cole parameters were expressed as a linear function of the amount of glucose in the sample. The coefficients for each phantom are shown in Table VII. An example of the linear fitting for $\Delta\varepsilon_n$ parameter is plotted in Fig 12.

After the linear fitting, the trends of the Cole-Cole parameters were examined; apart from ε_∞ and σ_i, all the parameters demonstrate a decreasing trend with the increase in the dextrose levels. The ε_∞ trend is slightly increasing, whereas σ_i remains almost constant while the dextrose levels are increasing. The trend observed for ε_∞ and $\Delta\varepsilon_n$ agrees with previously published results [24]. The increase of ε_∞ with dextrose content implies that an increase in relative dielectric

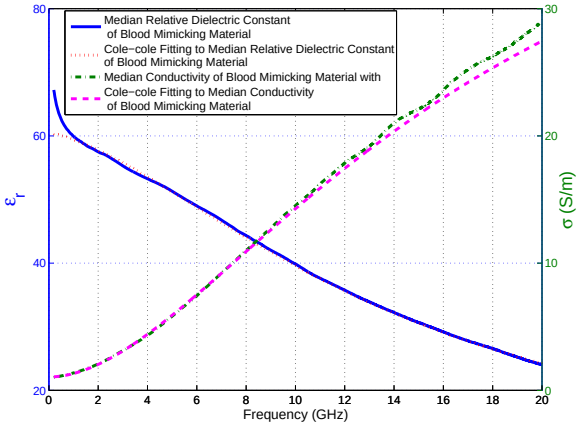

Fig. 11. Comparison between the median of the dielectric property measurement and Cole-Cole fitting performed for blood mimicking material with 0 g of dextrose.

TABLE VII
COEFFICIENTS OF THE LINEAR FUNCTION $y = ax + b$ FITTED TO COLE-COLE PARAMETERS WITH RESPECT TO GLUCOSE CONCENTRATION

Coefficient	ε_∞	$\Delta\varepsilon_n$	τ_n (ps)	α_n	σ_i (S/m)
a	0.795	−1.953	−1.218	−0.113	0.011
b	2.86	57.93	11.28	0.084	1.05

constant is expected at high frequencies. From Fig. 12, the relative dielectric constant is expected to vary by approximately 1 unit when the minimum and maximum levels of glucose are considered. The τ_n parameter displays only minor variation with differing glucose index. Finally, from the analysis of the σ_i parameter, no significant changes in the conductivity of the phantoms are expected for minimum and maximum glucose content.

C. Patch Resonator Measurement Results with Four-Layered Tissue Mimicking Phantom

An S-parameter measurement in air media was performed, to verify the proper functioning of the resonator. Results

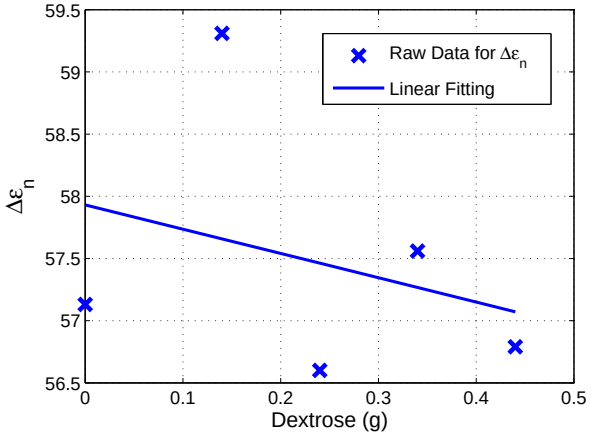

Fig. 12. Linear fitting to the $\Delta\varepsilon_n$ variable with respect to dextrose levels.

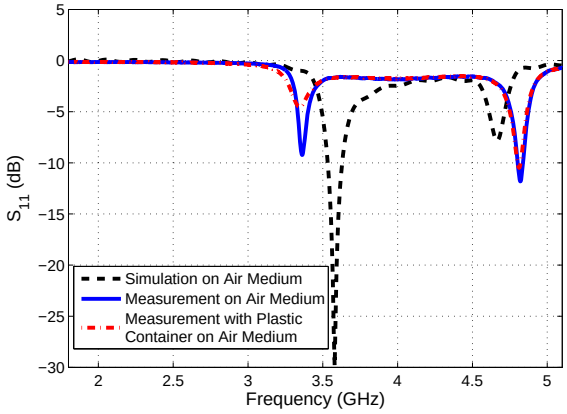

Fig. 13. Measured and simulated return loss of the resonator in air media.

from simulation in air media, measurement in air media, and measurement in air media with the resonator mounted at the bottom of the container are shown in Fig. 13. The difference between measured and simulated air media results shows that resonance shifts occurred due to the fabrication process. Namely, the first notch is shifted 216 MHz to left and the second notch 218 MHz to right. Additionally, due to the plastic box, the first notch shifts 17 MHz to left and the second notch shifts 70 MHz to right. The overall difference between simulation and mounted resonator performance is 233 MHz to left and 148 MHz to right, for first and second notches, respectively.

The simulated and measured return loss of the resonator with the four-layered tissue mimicking phantom are shown in Fig. 14. Note that the blood layer has no dextrose. The simulated resonance frequency is 2.451 GHz, whilst the measured resonance frequency is 2.143 GHz. The measured resonance frequency is shifted to the left by 308 MHz, when compared with the simulation. From Fig. 13, the first notch is shifted to the left by 233 MHz due to fabrication and plastic (polypropylene) container, since the plastic container was not included in the simulations. The relative dielectric constant of polypropylene is 2.2 and the dissipation factor is 0.0003 at 1 GHz. The other factors that can affect the resonance frequency include the mismatch in relative dielectric constant and conductivity of the physical phantoms with respect to human tissues. Note that non-frequency-dispersive digital phantoms were considered during the simulation, using the dielectric properties at 2.45 GHz (shown in Table III), whereas the physical phantoms used in the experiments were frequency-dispersive.

Next, the blood layer without dextrose was exchanged with the blood layers with higher dextrose content in turn, and the S-parameter response of the resonator collected. Seven measurements were taken for each blood layer, 28 measurements taken in total. Then, the median of S-parameter response for each dextrose level is taken to calculate the input impedance for each glucose level. The results are also shown in Fig. 15. From the Cole-Cole parameter results, a maximum change in the relative dielectric constant of the blood layer of 1 unit is

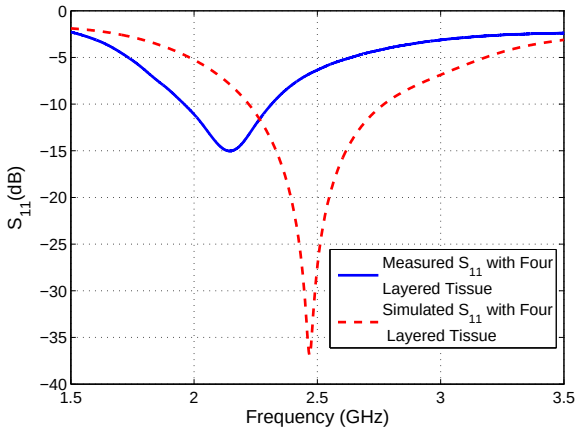

Fig. 14. Measured and simulated return loss of the resonator with four-layered tissue mimicking material.

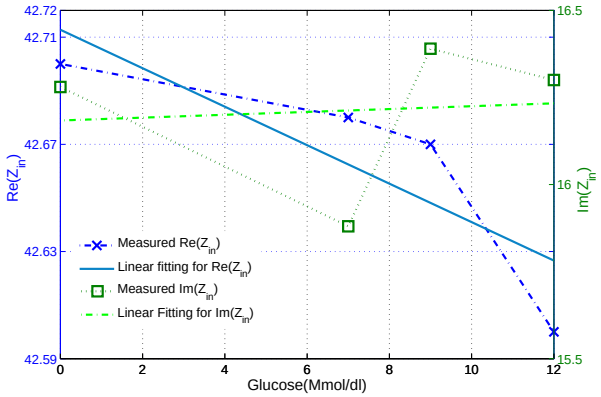

Fig. 15. Measured input impedance with four-layered tissue mimicking material by alternating the blood layer with four different glucose indices.

expected.

In Fig. 6, a 1 unit change in the relative dielectric constant of the blood layer corresponds to a $+0.2\ \Omega$ and $-0.02\ \Omega$ change in the real and imaginary parts of the input impedance, respectively. Fig. 15 shows the calculated input impedance from the measured S-parameter results at the resonance frequency. The change in the real and imaginary part of the input impedance is $-0.08\ \Omega$ and $+0.05\ \Omega$, respectively.

The discrepancy between the measurement and simulations could be due to the resonance frequency shift in the measurement, when compared to the simulation. Another reason for the discrepancy could be due to the thickness differences between the physical BMM layers with different glucose indexes. The layers are fabricated by marking 2.5 mm height on the identical containers and pouring liquid BMM. The process is repeated for each BMM with different glucose index. However, 2.5 mm is a very small thickness and, although meticulous attention was paid to the thickness of the BMM during the experiments, the authors suspect that the thickness of the BMM layers might have slight differences. Such differences in thickness can effect the response of the resonator.

This effect was investigated by simulating the proposed patch resonator loaded with a four layered tissue mimicking material, where the digital BMM layer's thickness ranged from 0.5 mm to 5.5 mm at 9 different points. From the simulated S-parameter response, the thickness dependence of the input impedance was calculated. The results at the resonance frequency are shown in Fig. 16. As the thickness increases, the input impedance decreases, as expected: changing the dimensions of each layer changes the effective permittivity, thus changing the matching of the resonator.

As this work represents an initial study, there is still a need to perform additional measurements within the realistic BGL range, to provide a baseline for further studies. In particular, the experiment will be repeated with smaller glucose index values, to identify the minimum detectable glucose index with the patch resonator; this is important for hypoglycemia, for example. In addition, the step size in glucose index values should be reduced and more data points should be collected, to further verify the initial results shown above. The maximum glucose level can also be increased, to allow for the response to extreme values (e.g., in hyperglycemia) to be determined. These experiments must also be performed with more sensitive resonators.

It is apparent that the realistic changes in BGL (i.e., restricted to a narrow range) result in restrictions in the degree of change in the measurable dielectric properties. Whilst this study has demonstrated laboratory-level measurements can still detect the observable changes, this is a long way from practical applications, especially when considering that other physiological processes can produce similar, or even larger, changes in the dielectric properties.

Additionally, the layered superstrate geometry proposed in this paper is not claimed to be fully representative of the complex human tissue. The blood layer has been considered as a homogeneous layer, whereas blood is actually encased within vessels and heterogeneously distributed within the tissues. However, producing an anthropomorphic physical phantom is extremely challenging and is likely only possible with advanced fabrication techniques not readily available. It is also noted that even the major blood vessels will have subject-specific variation in their dimensions and location within the tissues, introducing further uncertainties. Hence, the simplified model was selected as a means of achieving the two primary goals of this work: developing wide-band TMPs and using those TMPs to investigate resonator sensitivity to the realistic blood glucose levels.

In addition, in order to simulate a more realistic superstrate (including the use of blood vessels), a very high resolution digital human phantom must be employed. Although digital phantoms capable of discriminating the smallest blood vessels are not readily available, there are voxelized models with fairly good resolution which can be used in electromagnetic simulation software. However, the computational burden is significantly higher and there can be issues related to the position of the resonator and the 'stair-casing' of the body surface. For this study, it was decided to focus on the simplified model, as this would allow direct comparisons with the experiments deemed suitable and achievable, as discussed above.

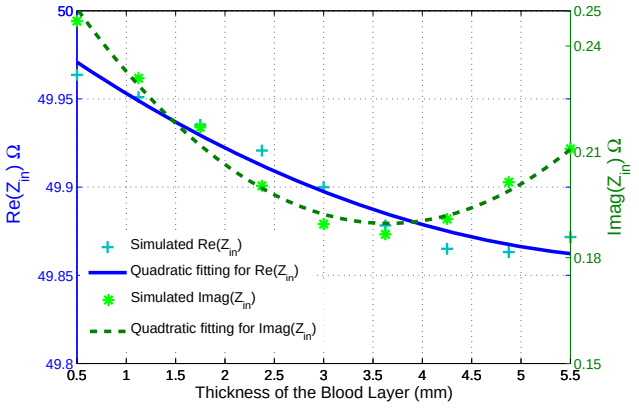

Fig. 16. Simulated input impedance of patch resonator with four-layered digital tissue mimicking material with different digital blood layer thickness.

Also, it should be noted that the glucose levels do not only change in the blood. Glucose is distributed to cells throughout the body, in all tissues, via the circulatory system. In particular, it is known that the glucose levels in the interstitial tissue fluid also vary throughout the day. Thus, such changes in the glucose levels are expected to affect the dielectric properties of other tissues, such as muscle and fat, as well as the interstitial tissue fluid itself. Hence, the real relationship between changing glucose levels and changing effective permittivity is extremely complex and requires a great deal of further research. However, despite the simplification of the complex human tissue made in this work, it is believed that the results above are useful to set the boundaries of what must be detected, allowing the resonator performance to be specified.

Typically, resonators are specified in terms of their operating frequency and bandwidth; an alternative figure-of-merit to bandwidth is the quality factor (Q-factor, or Q). One method for estimating the total Q is using

$$\frac{\Delta f}{f_r} = \frac{\text{VSWR} - 1}{Q_t \sqrt{\text{VSWR}}} \tag{4}$$

where f_r is the resonant frequency, Δf is the operating bandwidth for the resonator and VSWR is the voltage standing wave ratio level used to determine the relevant bandwidth. Low-Q resonators thus have wide bandwidths and correspondingly low frequency selectivity; high-Q resonators have narrow bandwidths and high selectivity. The total Q is affected by various losses in the system, some of which are unavoidable (in particular, the losses in the tissues).

It is obvious that a high-Q resonator would be preferred to measure BGL, given the narrow variation of dielectric properties related to normal variations in BGL (and resulting small changes in resonant frequency and input impedance magnitude). The total Q of the patch resonator used in this study is estimated using (4) as Q_t =4.0653, for a VSWR of 1.92 (this is equivalent to $S_{11} = -10$ dB) and f_r =2.143 GHz. The lower and upper limits of the resonant band are 1.962 GHz and 2.312 GHz, respectively. Hence, this resonator is low-Q and not optimal for this application. Higher-Q resonators will be investigated to improve performance. It is also worth noting that resonators operating at higher frequencies can provide higher Q-values for the same absolute bandwidth Δf. This provides two avenues for investigation: higher frequency operation, which may have limitations related to penetration of the RF signal into the body tissue, and resonator designs with inherently higher Q, which are likely to be more complex in geometry, or fabrication, or both.

V. Conclusions and Future Work

In this paper, recipes and dielectric property measurements for wide-band tissue mimicking materials were presented, for four tissues: muscle, fat, blood and wet skin. One objective was to make wide-band physical phantoms that allow experimental validation of simulations in future studies; a second was to use these TMPs in investigations of more realistic levels of blood sugar, allowing the poorly-understood trade-offs regarding the RF resonator (size, sensitivity, operating frequency) to be examined. The results presented demonstrate that wide band phantoms were developed that were comparable, or better than, similar phantoms for these tissues, whilst using readily-available and cheap ingredients.

This paper also presents dielectric spectroscopy results of the blood mimicking material with realistic blood glucose levels. The results of the dielectric spectroscopy suggest that there is only a slight change in the relative dielectric constant of the blood with altering realistic glucose levels and the conductivity is expected to remain constant. This information provides some initial insight into the sensitivity issues that will be faced when trying to use RF techniques to monitor (and, ideally, control and keep within) realistic blood glucose levels.

To further investigate these issues, the wide-band TMP materials were used in measurements performed with a patch resonator, with varying quantities of dextrose added to the blood layer. This work examined the possibility of measuring the blood glucose levels non-invasively and continuously within the realistic blood glucose level range. It has been shown that the input impedance response of the patch resonator is sensitive to the changes in the relative dielectric constant of the blood layer. The trend of the measured input impedance has been shown to be consistent with the simulated response. The proposed approach has potential for non-invasive continuous monitoring of changes in blood glucose level.

This work is on-going, with a number of areas requiring further study. This includes: refinement of the phantom recipes to reduce the error, especially at higher frequencies; including a greater range of dextrose values in the dielectric spectroscopy study, in order to improve the fit of the Cole-Cole model parameters as they vary with sugar level; and an investigation into the trade-offs for RF resonators, in the light of the new knowledge gained in this work. This latter includes a more detailed study of the response of the resonator to BGL changes and looking at higher resonant frequencies, or higher Q-factor resonators, or both. The simplified model phantom would be employed initially in developing the higher-Q resonators, with simulations using the voxelized human body models performed for further optimisation and verification. Of course,

to fully explore the possibilities, further analysis must also be carried out with human subjects at some suitable point. Other work includes an examination into the lifetimes of the phantoms and a study of their homogeneity, amongst other things.

APPENDIX

Detergent$_1$ is available in North America: a dishwashing liquid sold under the name of "Ultra Ivory". Detergent$_2$ is available in United Kingdom: a dishwashing liquid called "Fairy Platinum Lemon". From Fig. 17, it is shown that relative dielectric constant of the detergent$_1$ is approximately 10 units higher than the detergent$_2$ over the frequency range of 0.3 GHz to 20 GHz, and the conductivity of detergent$_1$ is higher than detergent$_2$. The dielectric properties of the fat mimicking material is very low; thus, detergent$_2$ is preferred for the fat mimicking material. Any dishwashing liquid can be used in place of detergent$_1$ and detergent$_2$; however, it is recommended to measure the dielectric properties before doing so, to obtain precise dielectric properties in the phantom.

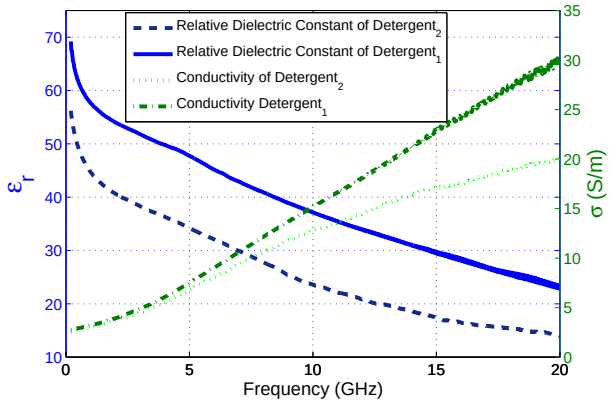

Fig. 17. Measured dielectric properties of detergent$_1$ and detergent$_2$.

REFERENCES

[1] National Health Services. URL: http://www.dh.gov.uk.

[2] T. Karacolak, A. Hood, and E. Topsakal, "Design of a dual-band implantable antenna and development of skin mimicking gels for continuous glucose monitoring," *Microwave Theory and Techniques, IEEE Transactions on*, vol. 56, no. 4, pp. 1001 –1008, april 2008.

[3] T. Karacolak, R. Cooper, and E. Topsakal, "Electrical properties of rat skin and design of implantable antennas for medical wireless telemetry," *Antennas and Propagation, IEEE Transactions on*, vol. 57, no. 9, pp. 2806 –2812, sept. 2009.

[4] M. Ahmadi and G. Jullien, "A wireless-implantable microsystem for continuous blood glucose monitoring," *Biomedical Circuits and Systems, IEEE Transactions on*, vol. 3, no. 3, pp. 169 –180, june 2009.

[5] B. Jean, E. Green, and M. McClung, "A microwave frequency sensor for non-invasive blood-glucose measurement," in *Sensors Applications Symposium, 2008. SAS 2008. IEEE*, feb. 2008, pp. 4 –7.

[6] E. C. Green, "Design of a microwave sensor for non-invasive determination of blood-glucose concentration," Master's thesis, Engineering and Computer Science, Baylor University, 2005, mentor: B. Randall Jean. [Online]. Available: http://beardocs.baylor.edu/xmlui/handle/2104/3000

[7] B. Freer and J. Venkataraman, "Feasibility study for non-invasive blood glucose monitoring," in *Antennas and Propagation Society International Symposium (APSURSI), 2010 IEEE*, july 2010, pp. 1 –4.

[8] Y. Hayashi, L. Livshits, A. Caduff, and Y. Feldman, "Dielectric spectroscopy study of specific glucose influence on human erythrocyte membranes," *Journal of Physics D: Applied Physics*, vol. 36, no. 4, pp. 369–374, 2003. [Online]. Available: http://stacks.iop.org/0022-3727/36/i=4/a=307

[9] Fogh-Andersen, Niels and DOrazio, Paul and Kuwa, Katsuhiko and Klpmann, Wolf R. and Mager, Gerhard and Larsson, Lasse, "Recommendation on reporting results for blood glucose," *eJIFCC*, vol. 12, no. 4, 2009, iFCC Scientific Division Working Group on Selective Electrodes. [Online]. Available: http://www.ifcc.org/ifccfiles/docs/vol12no4a4.pdf

[10] E. Topsakal, E. C. Moreland, T. Karacolak, and M. Acar, "The impact of glucose concentration in blood plasma on relative dielectric constant and conductivity," in *National Science Meeting URSI*, 2008.

[11] J. Venkataraman and B. Freer, "Feasibility of non-invasive blood glucose monitoring: In-vitro measurements and phantom models," in *Antennas and Propagation (APSURSI), 2011 IEEE International Symposium on*, july 2011, pp. 603 –606.

[12] K. Beam and J. Venkataraman, "Phantom models for in-vitro measurements of blood glucose," in *Antennas and Propagation (APSURSI), 2011 IEEE International Symposium on*, july 2011, pp. 1860 –1862.

[13] T. Yilmaz, T. Karacolak, and E. Topsakal, "Characterization of muscle and fat mimicking gels at mics and ism bands (402 mhz 405 mhz) and (2.4 ghz 2.48 ghz)," in *The XXIX General Assembly of the International Union of Radio Science*, August 2008.

[14] A. Mashal, F. Gao, and S. C. Hagness, "Heterogeneous anthropomorphic phantoms with realistic dielectric properties for microwave breast imaging experiments," *Microwave and Optical Technology Letters*, vol. 53, no. 8, pp. 1896–1902, 2011. [Online]. Available: http://dx.doi.org/10.1002/mop.26128

[15] P. S. Hall and Y. Hao, *Antennas and Propagation for Body-Centric Wireless Networks*. Artech House, 2006, iSBN 1-58053-493-7.

[16] T. Yilmaz, T. Karacolak and E. Topsakal, "Characterization and testing of a skin mimicking material for implantable antennas operating at ism band (2.4 ghz-2.48 ghz)," *Antennas and Wireless Propagation Letters, IEEE*, vol. 7, pp. 418 –420, 2008.

[17] T. Yilmaz and Y. Hao, "Electrical property characterization of blood glucose for on-body sensors," in *Antennas and Propagation (EUCAP), Proceedings of the 5th European Conference on*, april 2011, pp. 3659 –3662.

[18] M. Lazebnik, E. L. Madsen, G. R. Frank, and S. C. Hagness, "Tissue-mimicking phantom materials for narrowband and ultrawideband microwave applications," *Physics in Medicine and Biology*, vol. 50, no. 18, p. 4245, 2005. [Online]. Available: http://stacks.iop.org/0031-9155/50/i=18/a=001

[19] C. Gabriel, S. Gabriel, and E. Corthout, "The dielectric properties of biological tissues: I. literature survey," *Physics in Medicine and Biology*, vol. 41, no. 11, p. 2231, 1996. [Online]. Available: http://stacks.iop.org/0031-9155/41/i=11/a=001

[20] S. Gabriel, R. W. Lau, and C. Gabriel, "The dielectric properties of biological tissues: Ii. measurements in the frequency range 10 hz to 20 ghz," *Physics in Medicine and Biology*, vol. 41, no. 11, p. 2251, 1996. [Online]. Available: http://stacks.iop.org/0031-9155/41/i=11/a=002

[21] A. Peyman and C. Gabriel, "Colecole parameters for the dielectric properties of porcine tissues as a function of age at microwave frequencies," *Physics in Medicine and Biology*, vol. 55, no. 15, p. N413, 2010. [Online]. Available: http://stacks.iop.org/0031-9155/55/i=15/a=N02

[22] S. Gabriel, R. W. Lau, and C. Gabriel, "The dielectric properties of biological tissues: Iii. parametric models for the dielectric spectrum of tissues," *Physics in Medicine and Biology*, vol. 41, no. 11, p. 2271, 1996. [Online]. Available: http://stacks.iop.org/0031-9155/41/i=11/a=003

[23] M. Lazebnik, M. C. Converse, J. H. Booske, and S. C. Hagness, "Ultrawideband temperature-dependent dielectric properties of animal liver tissue in the microwave frequency range," *Physics in Medicine and Biology*, vol. 51, no. 7, p. 1941, 2006. [Online]. Available: http://stacks.iop.org/0031-9155/51/i=7/a=022

[24] E. Topsakal, T. Karacolak, and E. Moreland, "Glucose-dependent dielectric properties of blood plasma," in *The XXX General Assembly of the International Union of Radio Science*, August 2011.

[25] A. Hood and E. Topsakal, "Particle swarm optimization for dual-band implantable antennas," in *Antennas and Propagation Society International Symposium, 2007 IEEE*, june 2007, pp. 3209 –3212.

[26] M. Lazebnik, D. Popovic, L. McCartney, C. B. Watkins, M. J. Lindstrom, J. Harter, S. Sewall, T. Ogilvie, A. Magliocco, T. M. Breslin, W. Temple, D. Mew, J. H. Booske, M. Okoniewski, and S. C. Hagness, "A large-scale study of the ultrawideband

microwave dielectric properties of normal, benign and malignant breast tissues obtained from cancer surgeries," *Physics in Medicine and Biology*, vol. 52, no. 20, p. 6093, 2007. [Online]. Available: http://stacks.iop.org/0031-9155/52/i=20/a=002